Tree Seed Algorithm-Based Optimized Deep Features Selection for Glaucoma Disease Classification

Sherif Tawfik Amin
Department of Computer Science-College of Engineering and Computer Science, Jazan University, Jazan, Saudi Arabia

Abstract*—Glaucoma is a common eye condition that can cause irreversible blindness if left untreated. Glaucoma can be identified by the optic nerve disorder (a perilous path that carries the potential risk) and leads to blindness. Therefore, early glaucoma detection is critical for optimizing treatment outcomes and preserving vision. The majority of afflicted people typically do not exhibit any overt symptoms. Since many afflicted people go untreated as a result, early detection is essential for successful therapy. Systems for detecting glaucoma have been developed through a great deal of research. These manual, time-consuming, and frequently erroneous traditional diagnostic methods are not suitable for glaucoma diagnosis thus, automated methods are required. This research study proposes a novel glaucoma diagnosis model that addresses the difficulty of determining the complex cup-to-disc ratio. For accurate feature extraction, a publicly available dataset with two classes (Glaucoma positive and negative) is utilized from Kaggle. The dataset is augmented using the Flip technique and resized. A two-step approach using the Mobilenetv2 model is used to extract features from positive and negative classes. Accurate features are selected with the help of Transfer Function Sequential Analysis (TSA). The enriched features are then classified using three different classifiers: Cubic SVM, Ensemble Subspace KNN, and Fine KNN. The experimental evaluation comprises 7 and 8 cross-validation folds. On 7 folds Ensemble Subspace KNN provides an accuracy of 97.33%, and on 8 folds Fine KNN provides the best accuracy of 97.92%.

***Keywords*—Deep learning; tree seed algorithm; feature extraction; mobilenetv2**

I. INTRODUCTION

Among all the causes of death across the world, glaucoma is one of the main causes of death. When the intraocular pressure inside the retina is increased then glaucoma is caused which is defined as neuro-degenerative eye in medical terms. Glaucoma is the second most common disease that results in complete blindness of patients if it is not detected at the early stages. It is also responsible for the reduction in the life spans of patients [1]. The degenerative disease of the eye that results in complete blindness of patients is glaucoma which is characterized by the loss of vision loss and progressive optic neuropathy. Due to an increase in pressure or the fluid inside the eye, the optic nerve of the retina is damaged leading to the destruction of the optic cup and the optic disc of an eye. As a result, the size of the optic cup is increased with the increased size of the optic disc [2]. Glaucoma is one of the prominent eye diseases across the globe. According to the report of WHO, on the world-wide level, approximately 4.5 million people suffer from complete blindness due to Glaucoma. This disease is developed by the gradual deterioration of the fibers of optic nerves that results in the structural changes of the optic nerve and reduces the rim of neuro-retina [3]. Glaucoma is defined as the loss of vision; if it's not detected at the early stage, it results in severe conditions of vision. This disease is common among people with an age range of 40-80 years and the prevalence of this disease in this age range is 3.54%. Hence, it is observed that among every 200 individuals, 40 individuals are affected with Glaucoma disease [4].

Glaucoma is a retina disease caused by the excessive amount of fluid inside the eye, resulting in damage to the optic nerve. When there is excessive fluid inside the human eye, the blood pressure increases, resulting in irreversible blindness [5]. Early stages identification of glaucoma is difficult, without thorough an eye examination because it frequently exhibits no symptoms. Currently, in the medical field diagnostic techniques such as imaging tests and functional evaluation tests are limited in terms of sensitivity and specificity. Optical coherence tomography provides detailed cross-sectional images of the retina; it excels in capturing structural alterations in the retinal layers, but it falls short in the early identification of functional loss. Glaucoma can be present in different ways with symptoms ranging from only mild or no noticeable symptoms to severe and irreversible damage, early detection of glaucoma is challenging [6]. For the diagnosis of glaucoma, a detailed examination of the optic nerve head, visual field testing, and tonometry are essential tests [7]. Early detection and intervention of glaucoma can significantly reduce the risk of glaucoma-related visual loss diseases. For early detection of glaucoma is necessary to implement innovative methods for screening, identifying, and diagnosing changes over time [8].

When retinal ganglion cells are lost, their axons gradually degenerate resulting in glaucoma, an eye illness that if left untreated, can cause permanent vision loss. This disease affects 80 million people worldwide at various ages, and in 2020 it was anticipated to be the leading cause of blindness [9]. Fig. 1 describes the fundus images of glaucoma where (a) mentions the labeled image of the fundus or glaucoma and (b) mentions the detailed image of fundus for the analysis by medical practitioners.

Manual feature extraction is necessary for machine learning-related models, and it takes a lot of time and effort. Rather than requiring users to manually extract features from the data, deep learning techniques seek to examine more abstract features from the data [3]. The human community is said to favor science and technology. There are enormous expectations for reliable computer-aided systems (CAD) all around the world [4]. There are two basic groups into which glaucoma types can be divided: primary angle-closure and open-angle glaucoma [5]. However, there are still certain drawbacks, such as severe artifacts, poor image quality, reconstruction errors, pixel imbalance between the affected area and background, and low glaucoma detection sensitivity, all of which need to be found and fixed. Therefore, the goal is to provide a precise classification model for fundus image-based glaucoma detection. The main contributions of the proposed work are listed below as:

- In the proposed model, the complexity of identifying the cup-to-disc ratio for glaucoma detection has been overcome. To overcome this challenge, enhancement and resizing of images id performed for the expansion of the dataset. This process ensures accurate feature recognition, compensating for complex structures that make cup-to-disc ratios difficult to recognize.
- An accurate understanding of the glaucoma cup-to-disc ratio is achieved by extracting features from both positive and negative classes using a pre-trained model called Mobilenetv2, after that significant features get selected with the help of TSA.
- These features are fed to machine learning classifiers Cubic SVM, Ensemble Su space KNN, and Fine KNN.

The paper is arranged as: Section II describes Related Work, Section III describes Proposed Methodology, Section IV illustrates Results and Experiments, and Section V discusses Conclusion and Future Work.

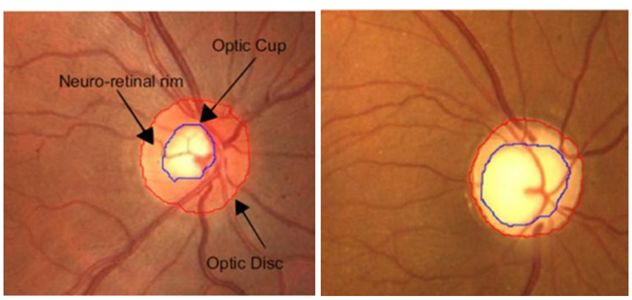

(a) (b)

Fig. 1. (a) Labeled image of Fundus (b) Detailed image for medical analysis [2].

II. LITERATURE REVIEW

The researchers utilized many Machine learning and deep learning methods [1, 6-19] strategies in various domains. A multi-branch neural network model is suggested for glaucoma diagnosis. Based on experimental findings, the constructed model reached 0.9151, 0.9233, and 0.9090 for accuracy, sensitivity, and specificity, respectively [20]. For the diagnosis of Glaucoma, the basic classification model CNN was utilized and amended where there were three convolution layers and one flattened layer. With the use of the least number of tunable parameters, the model learned and extracted the deep features of the images. PCA and LDA algorithms were applied to reduce the irrelevant feature and then the classification was performed in the final step [21]. To detect glaucoma, the deep learning models were utilized with the pre-trained models like MobileNet, DenseNet169, Xception, InceptionV3, VGG19, and ResNet152V2 [22]. A novice model of deep learning by using the OCT images of glaucoma was developed for the diagnosis of glaucoma. For efficient results, pre-trained vision transformer technology is applied on the eye dataset by extracting the features on the slice-based extraction, and then Gated Recurrent units were also utilized on the dataset [23]. Different unprocessed fundus images were trained by integrating hybrid ML and DL techniques for the recognition of glaucoma. For feature extraction, VGG was utilized and for classification, different models like AdaBoost, SVM, KNN, RF, and MLP were used [24]. During the diagnosis of glaucoma disease, an error that mostly occurs is the imbalanced data and to avoid this error, MAS Block architecture and many other image augmentation techniques were employed [25]. A simple CNN model was utilized for considering all the architectural designs of the fundus images for the detection of the disease. The pre-trained models of deep learning were applied for the classification purpose and the models included VGG16, ResNet50, AlexNet, and InceptionV3 [26]. YOLOv7 architecture i.e. an accurate and robust DL automated system was developed for the detection of glaucoma. This architecture was used to detect the optic cup and optic disc from the fundus images [27]. The disease of glaucoma disease can be identified by extracting features of the neuro-retinal rim using histogram and GLCM of the normal images of eye and the images with glaucoma disease. The process of feature extraction was carried out in three steps, firstly the acquisition of images was performed, secondly preprocessing was carried out and at the last step classification was performed [28]. The vision transformer for the object detection from the images was extended for the detection of glaucoma from the fundus images. The detection was carried out to calculate the cup-to-disc ratio of the eye and then analyze the neuro-retinal rim thinning on vertical alignment [29]. A novice heuristic-based UNet-Inception attention framework was developed for the classification and segmentation of optic nerves of eyes (glaucoma). Along with the fusion of UNet and Inception, Haris Hawks techniques were used for the selection of suiTABLE features with a hybrid loss function [30].

The fundus images of glaucoma were segmented by applying DL ensemble methods like GNet and UNet and these methods were integrated for the detection of the disease. Different preprocessing steps were involved for the accurate detection of the disease, the steps included normalization, resizing of images, contrast enhancement, and filtering for the optimization of the dataset image quality [31]. The disease of glaucoma can be detected by calculating the optic cup-to-disc ratio and to calculate this ratio a Joint U N net++ framework was developed that contained attention driven serial Unet++ based module features extraction, DDN, and CDN. The images were trained on ensemble networks of DarkNet19, EfficientNet-B1, and VGG19. For accurate results, the HBAS0GA algorithm was employed to optimize the results [32]. The classification of the fundus images of glaucoma was initiated first by the preprocessing of images, then blood vessels segmentation was performed, next features were extracted, and at the last step the classification of the eye diseases was performed. The classification was carried out by creating a hybrid classifier that integrated LRCN and SqueezeNet [33]. The fundus images classification was performed by applying the three different DL classifiers in which the first classified was used to control alterations against PAC, the second classified was used to control alterations against PACD, and the third classified was used to control alterations against PACS (PAC+PACG) [34].

Table I illustrates the detailed literature review of the research work carried out for the classification of glaucoma disease. The review comprises of the proposed method, the utilized dataset, the results achieved, and the future dimensions of the proposed method.

TABLE I. SUMMARY OF THE EXISTING METHODOLOGIES FOR THE CLASSIFICATION OF GLAUCOMA DISEASE

Author & Ref	Year	Proposed Method	Dataset	Results (Accuracy)	Limitations
Law Kumar Singh et al. [35]	2024	EPO + BFO	Fundus Images	96.55%	Applying EPO + BFO at later stages of assessments of patients
Ari Leshno et al. [36]	2024	ICD-10 Severity Classification + RS	Glaucoma Eye Dataset	15 true cases out of 18	Utilization of only functional information
Jeya Shyla N.S. et al. [37]	2024	UNet + KNN	Drishti GS1 & RIM-ONE	99.70%	Unable to enhance image boundaries sharpness
Marsida Bekollari et al. [38]	2024	Bayesian + PNN + SVM	Data from Opthamology Clinic of Elpis Geberal Hospital of Athens	81.10%	Lack of inappropriate combinations of features
Law Kumar Singh et al. [39]	2024	GSOA	Public & Private	95.36%	Comprehensive analysis of the datasets
Vijaya Kumar Velpula et al. [40]	2023	ResNet50+AlexNet+VGG19 +DenseNet-201+Inception_ResNet-v2	ACRIMA, RIM-ONE, HVD & Drishti	99.57% 85.43% 90.55% 95.95%	Real world implementation, larger dataset training
Sunija A.P. et al. [41]	2022	SD-OCT based depth wise separable convolution	Stanford Dataset	99.63%	Reduced model complexity
Thisara Shyamalee et al. [42]	2022	UNet+CNN+Inceptionv3+VGG19+ResNet50	RIM-ONE	99.58% 98.79%	Real time data implementation
Jahanzaib Latif et al. [43]	2022	ODGNet	ORFIS, HRF, DRIONS-DB, DR-HAGIS & RIM-ONE	95.75% 94.90% 94.75% 97.85%	Integration of automatic and handcrafted features
Ramgopal Kashyp et al. [44]	2022	UNet+DCNN+DensenNet-201	Glaucoma Dataset	98.82% 96.90%	Fuzzy and semi supervised models
Felix Joseph Xavier et al. [45]	2023	DeepLabv3+IROA	Standard Dataset	96.00%	-
Divya Gautam [46]	2024	FAWT+Text Features+PCA	RIM-ONE	96.21%	Complexity Reduction
Gavin D'Souza et al. [47]	2024	AlterNet-K Model	Rotterdam EyePACS AIROGS	91.60%	Larger Datasets and other domains
Charis Y.N. Chiang et al. [48]	2024	3D-CNN	Muscular tissues and ONH tissue scans	94.00%	Low Volume data
Abadh K Chaurasia et al. [49]	2024	CNN	Drsihti-GS1 & EyePACS	96.56%	Robust threshold technique

III. MATERIALS AND METHODS

In the proposed methodology, a two-step procedure is utilized for the classification of glaucoma disease. First, a pre-trained Mobilenetv2 model is used to enhance the feature extraction process from both positive and negative classes. By implementing a pre-trained model, it extracts powerful features from the dataset that capture essential patterns and characteristics. Then the retrieved features are refined by using the Tree Seed Algorithm (TSA), which is important for identifying relevant features, allowing for an attentive and selective subset that contains critical information for further analysis. The combination of effective and advanced feature selection with a robust pre-trained model creates a strong framework that enables the model to encapsulate significant information while reducing noise or inconsequential features. This overview provides a detailed examination of how a novel technique contributes to identifying complex patterns and representations inside different and complicated datasets and contributes to improving the overall model's efficacy and precision. The processed structure of the proposed methodology is illustrated in Fig. 2.

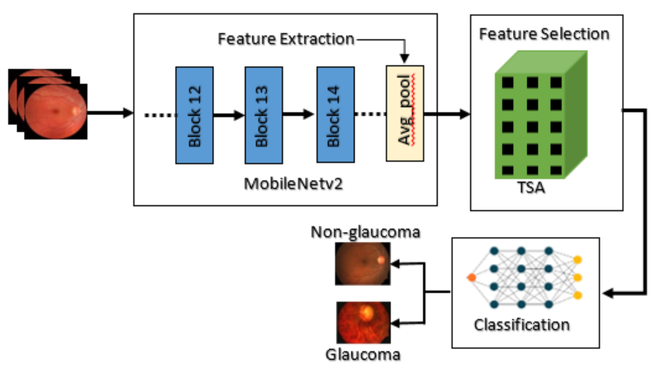

Fig. 2. Proposed MobTAS classification model.

Fig. 2 describes the architecture for the proposed methodology for the classification of Glaucoma images. The input images are fed into the MobileNetv2 classification model that is characterized by the consecutive blocks containing a back-to-back convolution layer, batch normalization layer, and ReLU layer thus comprising of total 19 residual blocks in which the convolution layers are present with the 32 filters. Then features are extracted from the fully connected layer of the model. The extracted features from the fully connected layer are then fed to the algorithm of TSFA for the selection of suitable features selection. Once the suiTABLE features are selected, those features are fed to three different classifiers: Cubic SVM, Fine KNN, and Ensemble Subspace KNN, and then the classification is performed.

A. Dataset Augmentation

Initially, the dataset consists of fewer images. Thus, to increase the number of samples, image augmentation is performed. Image augmentation is performed using the Flip (horizontal and vertical) technique as shown in Fig. 3.

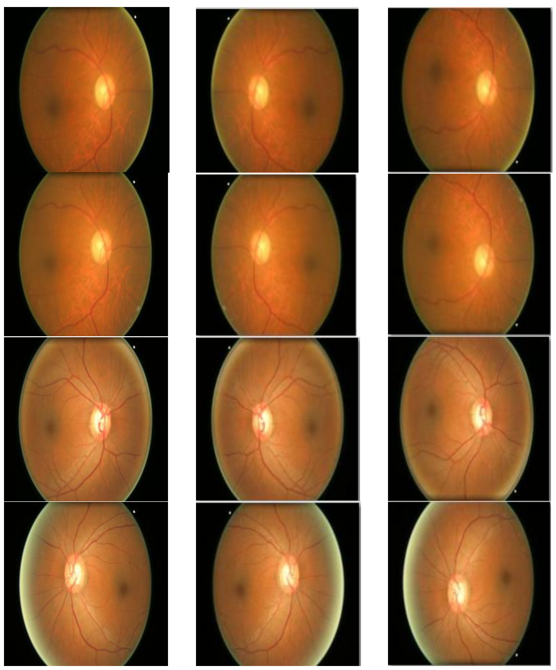

(a) (b) (c)

Fig. 3. Data augmentation (a) Original images (b) Horizontally flipped images (c) Vertically flipped images.

In Fig. 3 the results of data augmentation applied to the original images are represented. Data augmentation is performed to have enough number of images for training and testing of glaucoma dataset classification. Fig. 3 (a) represents the original images (b) represents the results of horizontal flip of images, and (c) represents the results of a vertical flip of images. All the original images and the augmented images are resized to size 224 x 224 for the accurate classification of the images.

B. Features Extraction

In the proposed method a pre-trained CNN model named Mobilenetv2 [43] that consists of 1632 connections and 154 layers is utilized to extract the deep features from the dataset. A feature vector with dimensions 1x1000 is methodically retrieved using the Mobilenetv2 model. The pre-trained model easily generates a 1x1000 feature vector, which acts as the starting point for subsequent studies. The critical features are detected and extracted from this extensive vector using the Tree Seed technique, an effective feature selection technique. This discriminative approach improves the model's ability to detect and prioritize significant features, maximizing efficacy for subsequent tasks. The intentional use of the Tree Seed algorithm demonstrates a diligent approach employed in refining the set of features. It ensures that Mobilenetv2 encapsulates significant features required for detailed evaluation, interpretation, and implementation in a wide range of computational tasks.

TABLE II. PARAMETERS USED IN CLASSIFICATION FOR FEATURES EXTRACTION

No. of epochs	10
Size of Input Images	224 x 224
No. of channels in images	03
No. of Filters	32
Seed Point	123
Batch Size	32
FBuffer Size	250
Fine Tune Point	125
Learning Rate	0.001
No. Dense Layers	64
Activation Function	ReLU
Dropout	0.25

Table II represents all the parameters that are selected and adjusted for the accurate classification and feature extraction of the available dataset images. These parameters are selected/adjusted on multiple turns of experiments and results.

C. Features Selection

The program TSA [50] which draws inspiration from nature, and provides the interaction between trees and their seeds for optimization. Finding a seed's position within tree is crucial to the optimization process. For this objective, the researcher proposes two searches in Eq. (1) and Eq. (2).

$$g\,(\vec{x}) \leq \; g\,(y) \qquad \forall\, \vec{y} \,\in G \tag{1}$$

$$g\,(\vec{x}) \geq \; g\,(y) \qquad \forall\, \vec{y} \,\in G \tag{2}$$

The first equation considers both the ideal site for the tree population and the tree location where the seed for this tree will be produced. Two distinct tree locations are used by the second update rule in Eq. (2) to generate a new tree seed.

$$Q_{i,j} = \; U_{i,j} + \propto_{i,j} \times (C_j + \; U_{r,j}) \tag{3}$$

$$Q_{i,j} = \; U_{i,j} + \propto_{i,j} \times (U_{i,j} + \; U_{r,j}) \tag{4}$$

where, $U_{i,j}$ is the jth dimension of ith tree, $Q_{i,j}$ is jth dimension of ith seed that will be produced ith a tree, C_j is the jth dimension of the best tree location obtained, $U_{r,j}$ is the jth dimension of rth tree randomly selected from the population in Eq. (3) and Eq. (4).

Using Eq. (5), the first tree sites that could be solutions to the optimization problem are generated at the start of the TSA search. This selection of location for new seed is controlled by a parameter known as search tendency (ST).

$$U_{i,j} = M_{j,min} + q_{i,j}\,(I_{j,max} - M_{j,min}) \quad (5)$$

$I_{j,max}$ is the upper bound of the search space, $M_{j,min}$ is the lower bound of the search space. In the interval [0, 1], a random number, denoted as $q_{i,j}$ is generated for every dimension and location. Using Eq. (6), the population's best solution is chosen for minimization.

$$C = \min\{g(\vec{U}_i)\}\; i = 1,2,3,\ldots,N \quad (6)$$

Where N is the population's total number of trees. (3) is used to update the dimension if a randomly generated number in the interval [0, 1] is less than ST; if not, Eq. (4) is applied.

D. Classification

For the classification of the disease of Glaucoma as either positive or negative, a pre-trained model MobileNetV2 is utilized that contains a total of 154 layers in which each convolutional layer has 32 filters. The convolution is performed by processing the images at each block and each convolutional layer. The features of the images are extracted from the last fully connected layer of the model and a feature vector is created that is further passed to TSA algorithm for the selection of the suiTABLE features. Once the suiTABLE features are selected, then the classification of the Glaucoma images is performed. Finally, classification based on the significant features is performed with the help of machine learning classifiers. In this phase, machine learning classifiers are used as a computational process to perform classification based on significant relevant features. The classification includes the robust Cubic Support Vector Machine (SVM) [51], renowned for ability to handle unpredicTABLE datasets and complex decision functions, the refined version of k-Nearest Neighbors (fine KNN) [52], known for proximity-based classification adaptability, and Ensemble subspace k-Nearest Neighbors (Ensemble Subspace KNN) [53, 54], which is a combination of combined learning and subspace techniques designed to perform well in complicated datasets. The implementation of various classifiers demonstrates an efficient methodology, ensuring model optimization for subtle pattern detection and correct classification in different and complicated data landscapes.

IV. Experimental Results

In the presented proposed methodology, a publicly available dataset is utilized. The glaucoma detection dataset [49] is downloaded from the Kaggle website. This dataset consists of two classes named glaucoma positive and glaucoma negative.

The dataset of glaucoma taken and utilized for the classification purpose in this paper is described in detail and the description is mentioned in Table III. The initial images in both classes were limited, so image augmentation is performed. To augment the original images, the flip technique (horizontal and vertical) is applied to the dataset after that all the images get resized. All the experiments and evaluations were conducted on MATLAB software using the Core i5 6th gen system. The designed method evaluated three machine learning classifiers including Cubic SVM, Ensemble subspace KNN, and Fine KNN on 7- and 8-folds cross-validation.

TABLE III. Description of Glaucoma Dataset

Dataset	Description
Glaucoma Detection	Type of Data: Eyes Images CT Scans of Eyes Format: .jpg Total images 500 Disease Depiction: Glaucoma Dimension of Images: 224 x 224 x 3 Channels: 3 Total Classes: 2

The results of the proposed model of Classification i.e. TSAMob are mentioned in Table IV where the model achieved an accuracy of 99.42%, loss of 0.0187%, validation accuracy of 84.85%, and validation loss of 2.2187%.

TABLE IV. Results of the Proposed Classification Model

Method	Accuracy	Loss	Validation Accuracy	Validation Loss
TSAMob	99.42%	0.0187%	84.85%	2.2187%

By applying a rigorous 7-fold cross-valid methodology, the proposed approach achieves a commendable overall accuracy using three distinct classifiers: 92.87% on Cubic Support Vector Machine (Cubic SVM), 97.33% on Ensemble Subspace k-Nearest Neighbors (Ensemble Subspace KNN), and 96.98% on Fine k-Nearest Neighbors (Fine KNN). These observations are mentioned in Table V. Unexpectedly, Ensemble Subspace KNN ranks as the best performer, with the highest accuracy across all the classifiers evaluated in this experimental work. This significant accuracy highlights Ensemble Subspace KNN's reliability and effectiveness in extracting complex correlations within the dataset, which enables advanced pattern recognition.

The extracted features are passed to three classifiers Cubic SVM, Ensemble Subspace KNN, and Fine KNN. Then the classification is performed, and results are recorded. These findings highlight how well the chosen classifiers can distinguish glaucoma, particularly Ensemble Subspace KNN, which excels accurate sorting of data points. This demonstrates effectiveness and reliability for applications requiring exact classification in a wide range of complicated data.

Table VI shows the experimental findings of the proposed approach by using the 8 folds cross-validation. When using an extended 8-fold cross-validation methodology. The Fine k-Nearest Neighbors (Fine KNN) ranks as the top classifier, with an outstanding accuracy of 97.92% In comparison with this Ensemble Subspace k-Nearest Neighbors (Ensemble Subspace KNN) achieves an accuracy of 96.94%, and Cubic Support Vector Machine (Cubic SVM) achieves 92.83% accuracy, respectively.

The extracted features are passed to three classifiers Cubic SVM, Ensemble Subspace KNN, and Fine KNN. Then the classification is performed, and results are recorded. The accuracy of Fine KNN demonstrates effectiveness while identifying complex patterns within the dataset; this makes it an effective application for requiring high precision.

In Table VII an extensive overview of the proposed technique with existing methodologies is provided. Notably, this comparison demonstrates that the suggested method performs excellently and gives the highest accuracy when compared with other alternative approaches. This difference makes the suggested model the best among all the other techniques in producing excellent results.

Fig. 4 shows the graphical presentation for the comparison of results obtained by the existing methodologies and the proposed methodology, and the proposed methodology has achieved better results.

In Fig. 5 the study shows the confusion matrix of the results obtained after the classification of the original dataset. Three classifiers are utilized for the feature extraction and classification and there are 7 folds cross validation (a) represents the confusion matrix of Cubic SVM Classifier, (b) represents confusion matrix of Ensemble Subspace KNN, and (c) represents the confusion matrix of Fine KNN.

TABLE V. PROPOSED METHOD RESULTS USING 7-FOLD CROSS VALIDATION

Classifier	Fold	Classes		Accuracy	Precision	Recall	F1 Score	Overall Accuracy
		Negative	Positive					
Cubic SVM	7	✓		92.87%	0.92	0.95	0.94	92.87%
			✓	92.87%	0.93	0.90	0.92	
Ensemble SubspaceKNN		✓		97.35%	0.96	0.99	0.98	**97.33%**
			✓	97.35%	0.99	0.95	0.97	
Fine KNN		✓		96.98%	0.96	0.99	0.97	96.98%

TABLE VI. PROPOSED METHOD RESULTS USING 8-FOLD CROSS VALIDATION

Classifier	Fold	Classes		Accuracy	Precision	Recall	F1 Score	Overall Accuracy
		Positive	Negative					
Cubic SVM	8	✓		92.83%	0.93	0.95	0.94	92.83%
			✓	92.83%	0.93	0.90	0.91	
Ensemble SubspaceKNN		✓		96.94%	0.96	0.99	0.97	96.94%
			✓	96.94%	0.99	0.94	0.96	
Fine KNN		✓		97.92%	0.97	0.99	0.98	**97.92%**
			✓	97.92%	0.99	0.96	0.98	

TABLE VII. COMPARISON OF PROPOSED METHOD WITH EXISTING TECHNIQUES ON DIFFERENT DATASETS

Ref#	Year	Method	Results (Accuracy)
[55]	2023	VGG19	88.5%
		InceptionV3	83.5%
		EfficientNetV1	87.5%
		MobileNetV2	88%
		AlexNet	90%
		Custom Layer	93%
[56]	2022	CNN with ResNet-34	94%
[57]	2019	AG-CNN	96.2%
Proposed	2023	Mobilenetv2+TSA+ Fine KNN	**97.92%**

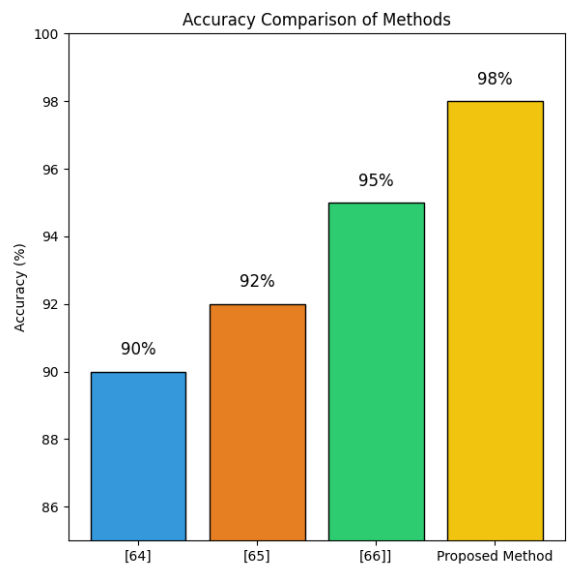

Fig. 4. Graph of results comparison between existing studies and the current study.

(a)

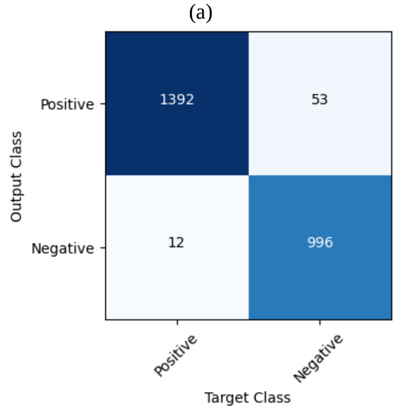

(b)

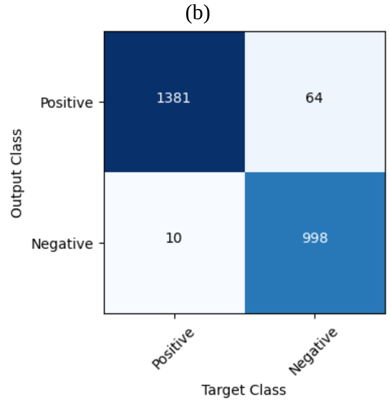

(c)

Fig. 5. Confusion matrix of three classifiers on 7 folds cross validation (a) Cubic SVM (b) Ensemble subspace KNN (c) Fine KNN.

V. Discussion

In this section, the discussion which concerns some ethical key including privacy of patient data, bias in algorithms, diagnostic transparency and the clinical accuracy of AI-assisted decision-making processes. This update will ensure a more comprehensive analysis of proper use of technology in medical applications.

VI. Conclusion

Automated glaucoma diagnosis plays a critical role in the early identification and management of the condition. Conventional techniques are laborious, tedious, and imprecise. This research proposes a model for the automatic classification of glaucoma stages. The prepared dataset (augmented and resized) was utilized for glaucoma classification into positive and negative classes. The features are extracted by Mobilenetv2, and significant features are selected using TSA. Using 7 folds Cross Validation, the Cubic SVM, Ensemble Subspace KNN, and Fine KNN provided the accuracy of 92.87%, 97.33%, and 96.98% respectively. On the 8 folds Cross Validation, the above-mentioned classifiers provided an accuracy of 92.83%, 96.94%, and 97.92% respectively. The results of the experiment show that the suggested model performs better than the most advanced techniques for glaucoma classification in the initial phases. This suggests that the model has an opportunity to improve glaucoma early detection and diagnosis, which can help avert vision loss and permanent blindness. Lastly, the suggested study may facilitate the prompt, accurate, and effective diagnosis of glaucoma by ophthalmologists.

The proposed methodology may be extended in the future by utilizing large real-time datasets of Glaucoma both on a manual basis and on clinical levels. The suggested automated glaucoma diagnostic model can be improved by more research in the following areas: real-world application, integration of clinical data, and larger datasets that provide generalization.

Funding

No applicable.

Informed Consent Statement

Not applicable.

Data Availability Statement

Publicly available.

References

[1] Adeel, A., et al., Diagnosis and recognition of grape leaf diseases: An automated system based on a novel saliency approach and canonical correlation analysis based multiple features fusion. 2019. 24: p. 100349.

[2] Diaz-Pinto, A., et al., CNNs for automatic glaucoma assessment using fundus images: an extensive validation. 2019. 18: p. 1-19.

[3] Sun, Y.J.I.A., The neural network of one-dimensional convolution-an example of the diagnosis of diabetic retinopathy. 2019. 7: p. 69657-69666.

[4] Mansour, R.F.J.B.e.l., Deep-learning-based automatic computer-aided diagnosis system for diabetic retinopathy. 2018. 8: p. 41-57.

[5] Zheng, W., et al., Systemic medication associations with presumed advanced or uncontrolled primary open-angle glaucoma. 2018. 125(7): p. 984-993.

[6] Ansari, G.J., et al., A novel machine learning approach for scene text extraction. 2018. 87: p. 328-340.

[7] Iqbal, Z., et al., An automated detection and classification of citrus plant diseases using image processing techniques: A review. 2018. 153: p. 12-32.

[8] Khan, M.A., et al., Lungs cancer classification from CT images: An integrated design of contrast based classical features fusion and selection. 2020. 129: p. 77-85.

[9] Lal, S., et al., Adversarial attack and defence through adversarial training and feature fusion for diabetic retinopathy recognition. 2021. 21(11): p. 3922.

[10] Liaqat, A., et al., Automated ulcer and bleeding classification from WCE images using multiple features fusion and selection. 2018. 18(04): p. 1850038.

[11] Nasir, I.M., et al., Deep learning-based classification of fruit diseases: An application for precision agriculture. 2021. 66(2): p. 1949-1962.

[12] Nasir, I.M., et al., Pearson correlation-based feature selection for document classification using balanced training. 2020. 20(23): p. 6793.

[13] Naz, M., et al., From ECG signals to images: a transformation based approach for deep learning. 2021. 7: p. e386.

[14] Nisa, M., et al., Hybrid malware classification method using segmentation-based fractal texture analysis and deep convolution neural network features. 2020. 10(14): p. 4966.

[15] Shah, J.H., et al., Facial expressions classification and false label reduction using LDA and threefold SVM. 2020. 139: p. 166-173.

[16] Sharif, M., et al., Human action recognition: a framework of statistical weighted segmentation and rank correlation-based selection. 2020. 23: p. 281-294.

[17] Zafar, M., et al., CNN Based Features Extraction and Selection Using EPO Optimizer for Cotton Leaf Diseases Classification. 2023. 76(3): p. 2779-2793.

[18] Zafar, M., et al., DeepLabv3+-based segmentation and best features selection using slime mould algorithm for multi-class skin lesion classification. 2023. 11(2): p. 364.

[19] Zafar, M., et al., Skin lesion analysis and cancer detection based on machine/deep learning techniques: A comprehensive survey. 2023. 13(1): p. 146.

[20] Chai, Y., H. Liu, and J.J.K.-B.S. Xu, Glaucoma diagnosis based on both hidden features and domain knowledge through deep learning models. 2018. 161: p. 147-156.

[21] Sharma, S.K., et al., An evolutionary supply chain management service model based on deep learning features for automated glaucoma detection using fundus images. 2024. 128: p. 107449.

[22] Patil, R., S.J.M.T. Sharma, and Applications, Automatic glaucoma detection from fundus images using transfer learning. 2024: p. 1-20.

[23] Ashtari-Majlan, M., M.M. Dehshibi, and D.J.a.p.a. Masip, Spatial-aware Transformer-GRU Framework for Enhanced Glaucoma Diagnosis from 3D OCT Imaging. 2024.

[24] C Gandhi, V., P.J.I.J.o.C. P Gandhi, and D. Systems, Glaucoma Eyes Disease Identification: Using Vgg16 Model throughDeep Neural Network. 2024. 16(1): p. 1-10.

[25] Khajeha, H.R., M. Fateh, and V. Abolghasemi, Diagnosis of glaucoma using multi-scale attention block in convolution neural network and data augmentation techniques. 2024.

[26] Govindan, M., et al., A Framework for Early Detection of Glaucoma in Retinal Fundus Images Using Deep Learning. 2024. 62(1): p. 3.

[27] Gao, X.R., et al., Automated vertical cup-to-disc ratio determination from fundus images for glaucoma detection. 2024. 14(1): p. 4494.

[28] Nugraha, G.S., et al., Glaucoma Detection Based on Texture Feature of Neuro Retinal Rim Area in Retinal Fundus Image. 2024. 1(3): p. 117-127.

[29] Chincholi, F. and H.J.F.i.A.I. Koestler, Transforming glaucoma diagnosis: transformers at the forefront. 2024. 7.

[30] Banerjee, T., G.S. Narula, and R. Wason, HHO-UNet-IAA: Harris Hawks Optimization based Novel UNet-Inception Attention Architecture for Glaucoma Segmentation. 2024.

[31] Meenakshi Devi, P., et al., Novel Methods for Diagnosing Glaucoma: Segmenting Optic Discs and Cups using Ensemble Learning Algorithms and CDR Ratio Analysis. 2024: p. 1-20.

[32] Mathew, J.C., et al., Joint Runet++: A Joint Region-Based Unet++-Based Optic Disc and Cup Segmentation with Ensemble Generalization Loss for Glaucoma Disease Prediction. 2024. 12(14s): p. 160-173.

[33] Alharbi, M.J.M.T. and Applications, Multi-classification of eye disease based on fundus images using hybrid Squeeze Net and LRCN model. 2024: p. 1-30.

[34] Shan, J., et al., Deep Learning Classification of Angle Closure based on Anterior Segment OCT. 2024. 7(1): p. 8-15.

[35] Singh, L.K., et al., Feature subset selection through nature inspired computing for efficient glaucoma classification from fundus images. 2024: p. 1-72.

[36] Leshno, A., et al., Improving glaucoma staging in clinical practice by combining the ICD-10 glaucoma severity classification system and optical coherence tomography. 2024. 38(1): p. 153-160.

[37] NS, J.S., W.S.J.M.T. Emmanuel, and Applications, Glaucoma stage classification using UNET-based segmentation with multiple feature extraction technique. 2024: p. 1-17.

[38] Bekollari, M., et al., Computer-Aided Discrimination of Glaucoma Patients from Healthy Subjects Using the RETeval PorTABLE Device. 2024. 14(4): p. 349.

[39] Singh, L.K., et al., Efficient feature selection based novel clinical decision support system for glaucoma prediction from retinal fundus images. 2024. 123: p. 104077.

[40] Velpula, V.K. and L.D.J.F.i.P. Sharma, Multi-stage glaucoma classification using pre-trained convolutional neural networks and voting-based classifier fusion. 2023. 14: p. 1175881.

[41] Sunija, A., et al., Redundancy reduced depthwise separable convolution for glaucoma classification using OCT images. 2022. 71: p. 103192.

[42] Shyamalee, T. and D.J.M.I.R. Meedeniya, Glaucoma detection with retinal fundus images using segmentation and classification. 2022. 19(6): p. 563-580.

[43] Latif, J., et al., ODGNet: a deep learning model for automated optic disc localization and glaucoma classification using fundus images. 2022. 4(4): p. 98.

[44] Kashyap, R., et al. Glaucoma detection and classification using improved U-Net Deep Learning Model. in Healthcare. 2022. MDPI.

[45] Xavier, F.J.J.C. and Systems, ODMNet: Automated glaucoma detection and classification model using heuristically-aided optimized DenseNet and MobileNet transfer learning. 2024. 55(1): p. 245-277.

[46] Gautam, D.J.M.T. and Applications, Improved machine learning-based glaucoma detection from fundus images using texture features in FAWT and LS-SVM classifier. 2024: p. 1-16.

[47] D'Souza, G., P. Siddalingaswamy, and M.A.J.B.E.L. Pandya, AlterNet-K: a small and compact model for the detection of glaucoma. 2024. 14(1): p. 23-33.

[48] Chiang, C.Y., et al., Are Macula or Optic Nerve Head Structures Better at Diagnosing Glaucoma? An Answer Using Artificial Intelligence and Wide-Field Optical Coherence Tomography. 2024. 13(1): p. 5-5.

[49] Chaurasia, A., et al., Highly accurate and precise automated cup-to-disc ratio quantification for glaucoma screening. 2024: p. 2024.01. 10.24301093.

[50] Ilham, M., et al., Experimenting with the Hyperparameter of Six Models for Glaucoma Classification. 2023. 9(3): p. 571-584.

[51] Singh, S. and R. Kumar. Histopathological image analysis for breast cancer detection using cubic SVM. in 2020 7th international conference on signal processing and integrated networks (SPIN). 2020. IEEE.

[52] Venkata Subbarao, M. and P.J.W.P.C. Samundiswary, Performance analysis of modulation recognition in multipath fading channels using pattern recognition classifiers. 2020. 115: p. 129-151.

[53] Bavkar, S., B. Iyer, and S. Deosarkar. Detection of alcoholism: An EEG hybrid features and ensemble subspace K-NN based approach. in Distributed Computing and Internet Technology: 15th International Conference, ICDCIT 2019, Bhubaneswar, India, January 10–13, 2019, Proceedings 15. 2019. Springer.

[54] Gul, A., et al., Ensemble of a subset of k NN classifiers. 2018. 12: p. 827-840.

[55] Ilham, M., et al., Experimenting with the Hyperparameter of Six Models for Glaucoma Classification. J. Ilm. Tek. Elektro Komput. dan Inform, 2023. 9(3): p. 571-584.

[56] Ramaida, F.M., K. Usman, and N.K.C. Pratiwi. Automatic Glaucoma Classification Using Residual Network Architecture. in Proceedings of the 2nd International Conference on Electronics, Biomedical Engineering, and Health Informatics: ICEBEHI 2021, 3–4 November, Surabaya, Indonesia. 2022. Springer.

[57] Li, L., et al., A large-scale database and a CNN model for attention-based glaucoma detection. IEEE transactions on medical imaging, 2019. 39(2): p. 413-424.